5. M. F. Weber and H. R. Shanks, *Natl. Bur. Std. Spec. Publ. 455*, Alan D. Franklin, Editor, p. 297, Government Printing Office, Washington, D.C. (1976).
6. R. J. Colton, A. M. Guzman, and U. Wayne Rabalais, *J. Appl. Phys.*, **49**, 409 (1978).
7. P. G. Dickens and R. J. Hurditch, in "Chemistry of Extended Defects in Non-Metallic Solids," L. Eyring and M. O'Keeffe, Editors, p. 555, Amsterdam-North Holland (1970).
8. Jean-Paul Randin, *This Journal*, **120**, 378 (1973).
9. J. Vondrak and J. Balej, *Electrochim. Acta*, **18**, 1017 (1973).
10. H. R. Shanks, *J. Cryst. Growth*, **13/14**, 433 (1972).
11. Z. Nagy and J. McHardy, *This Journal*, **117**, 1222 (1970).
12. M. F. Weber, Ph.D. Thesis, Iowa State University, Ames, Iowa (1977).
13. M. F. Weber, *IS Report*, **IS-4437** (1978).
14. J. McHardy, Ph.D. Thesis, University of Pennsyl-

vania, Philadelphia, Pa. (1972).
15. M. McHardy and P. Stonehart, in "Electrochemistry," Series 2, Vol. VI, A. D. Buckingham and J. O'M. Bockris, Editors, p. 171, Butterworths, London (1976).
16. S. Srinivasan and E. Gileadi, *Electrochim. Acta*, **11**, 321 (1966).
17. B. E. Conway and H. Anderstein-Kozlowska, *Natl. Bur. Std. Spec. Publ. 455*, A. D. Franklin, Editor, p. 107, U.S. Government Printing Office, Washington, D.C. (1976).
18. J. Vondrak and B. Alej, *Electrochim. Acta*, **20**, 283 (1975).
19. D. B. Sepa, D. S. Ovcin, and M. V. Vojnovic, *This Journal*, **119**, 1285 (1972).
20. R. J. Mannan, Ph.D. Thesis, University of Pennsylvania, Philadelphia, Pa. (1967).
21. G. Siclate. J. Chevrier, J. Lenoir, and C. Eyraud, *Compt. Rend.*, **C 277**, 227 (1973).

Semiconductor Electrodes

XXV. The p-GaAs/Heptyl Viologen System. Photoelectrochemical Cells and Photoelectrochromic Displays

Benjamin Reichman, Fu-Ren F. Fan, and Allen J. Bard*

Department of Chemistry, The Universtiy of Texas at Austin, Austin, Texas 78712

ABSTRACT

The photoreduction of aqueous solutions of 1,1'-diheptyl-4,4'-bipyridyl (heptyl viologen, HV^{2+}) bromide on p-GaAs was investigated. Under irradiation with light of wavelengths below 885 nm, the photoreduction of HV^{2+} to form a precipitate of violet HVBr occurs on p-GaAs at a potential of ~400 mV more positive than the reversible potential of the HV^{2+}/HVBr couple on Pt. Oxidation of HVBr back to soluble HV^{2+} occurs in the dark at more negative potentials. Photoelectrochemical low capacity storage cells based on this reaction with Cu, Ni, or $H_xNb_2O_5$ counterelectrodes were constructed. In such cells, under illumination, the p-GaAs electrode behaves as the cathode, a photovoltage develops, and current flows in the external circuit, while HVBr precipitates on the electrode surface, and the counterelectrode is oxidized. In the dark, the current flows in the opposite direction, the p-GaAs is the anode, and reduction occurs at the counterelectrode. Such a cell also produces an alternating electrical output under periodic illumination. Photoelectrochromic cells based on this reaction and utilizing simultaneous addressing with light and electrical signals are also proposed.

A number of photoelectrochemical (PEC) cells employing semiconductor electrodes for the conversion of radiant to electrical energy (liquid junction photovoltaic cells) have been described (1-17). Most have employed n-type semiconductors and have been used for the instantaneous production of electricity without chemical storage. The possibility of a photochargeable PEC cell using a third storage electrode or with production of soluble reactants has been discussed, however (8, 10-11). PEC cells employing p-type electrodes are less common (8-9, 15-17). Studies of aqueous systems with p-GaAs and p-GaP have been reported (15-16, 18), but the observed efficiencies of these were usually quite small and in many cases problems with electrode stability were encountered. Investigations of p-GaAs electrodes in acetonitrile solutions suggest good stability under strict water-free conditions (19).
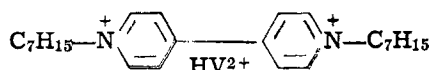
We report here investigations of the p-GaAs electrode immersed in aqueous solutions containing 1,1'-diheptyl-4,4'-bipyridyl (heptyl viologen, HV^{2+}) bromide. The reduction of HV^{2+} bromide on metal electrodes yields a precipitate of the violet radical cation

$$C_7H_{15}-\overset{+}{N}\langle\text{ }\rangle-\langle\text{ }\rangle\overset{+}{N}-C_7H_{15}$$
$$HV^{2+}$$

salt (Eq. [1]) and this has been suggested as the basis

$$HV^{2+} + Br^- + e \rightleftarrows HV^+ \cdot Br^- \qquad [1]$$
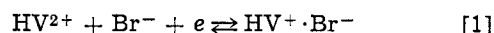
of electrochromic displays (20-22). The formation of such a precipitate by photoreduction at a p-type semiconductor would allow low capacity energy storage via a solid material, just as occurs in secondary batteries. We will show that such a photoreduction does occur at p-GaAs at potentials ~400 mV less negative than that observed at a platinum electrode and that dark oxidation of the HVBr precipitate is possible. Moreover, the p-GaAs electrode is stable both in the dark and under illumination in the HV^{2+} solution so that PEC cells using suitable counterelectrodes (*e.g.*, Cu/CuO) which show a periodic electrical output under chopped illumination can be constructed.

A second aspect of these studies concerns the application of reaction [1] on p-GaAs for display purposes. Several devices for active displays based on combining electrogenerated chemiluminescence and semiconductors have been described (23). A passive photoactivated display based on metal deposition on a semiconductor electrode was recently reported (24). The principles of a similar display based on precipitation of HVBr at a point on a semiconductor electrode simultaneously

addressed by light and an electrical signal is described here.

Experimental

The single crystal p-GaAs was obtained from Atomergic Chemicals (Long Island, New York) with acceptor concentration 3×10^{18} cm^{-3} (Zn-doped) and was mounted as an electrode as previously described (13). The surface (face 111) was first polished with 0.5 μm alumina powder and then etched for 10-15 sec in a solution which contained $H_2SO_4 : H_2O : 30\%$ H_2O_2 in concentration ratio 3:1:1. In some experiments single crystal p-GaP was also employed. The surface of this crystal was etched in 11M HCl for 10 sec before use.

As light sources either a 450W xenon lamp or a He-Ne laser (1.6 mW power) was used. The potentiostatic measurements were carried out with a Princeton Applied Research (PAR) potentiostat Model 173, with a cell consisting of an aqueous saturated calomel reference electrode (SCE) and a Pt wire as the counterelectrode. The electrochemical cell was provided with Pyrex windows for the passage of light. Nitrogen gas was passed through the solution before the experiments and above the solution during the experiments, since viologen radical cations are very sensitive to oxygen.

In the two electrode PEC cell experiments the voltage of the photocell between the p-GaAs and the oxide counterelectrode was measured on an x-t recorder through a voltage follower. The photocell current was measured on an x-t recorder through a current-to-voltage converter. For short time measurements of the cell short-circuit current, a Nicolet Model 1090A digital oscilloscope was used. The light intensity at the semiconductor surface was varied by means of neutral density filters.

Results

Cyclic voltammetry.—The i-V curve at a p-GaAs electrode of an unstirred solution of 0.01M HV^{2+} and 0.2M KBr at a scan rate of 100 mV/sec is shown in Fig. 1. In the dark (curve a) there was only a small current in the cathodic region with a very small peak on scan reversal. Under illumination of the p-GaAs electrode surface with the full power of the 450W xenon lamp, a larger cathodic current beginning at ~0.1V *vs.* SCE appeared (curve b). Simultaneously with the appearance of this cathodic current, the precipitation of the violet HVBr was observed on the electrode surface. On reversing the scan direction, a sharp anodic current peak occurred, either in the dark or under illumination. During the passage of the anodic current the violet precipitate on the semiconductor surface disappeared. Thus the overall process is that shown in [1], with illumination necessary for the reduction process, as is usual for p-type semiconductors.

These cyclic voltammograms could be repeated many (at least 100) times with only a small change in the peak height of the cathodic photocurrents, demonstrating good chemical reversibility of the deposition and stripping process. Upon illuminating the electrode with the narrow beam of a He-Ne laser, violet spots appeared on the electrode surface at exactly the location and of the size of the laser beam spot. The response time of the process was investigated by potential steps under illumination or by irradiation with chopped light with the electrode held at a constant potential (Fig. 2). A good coloration was observed on the electrode surface within ~0.5 sec after illumination of the electrode. Although the intensity ratio for HVBr deposited on dark p-GaAs is not very high, the deposition was easily discernable and this type of process can be considered for use as an electrochromic display controlled by both light and electrode potential and may also be applicable to photoimaging purposes (24, 25).
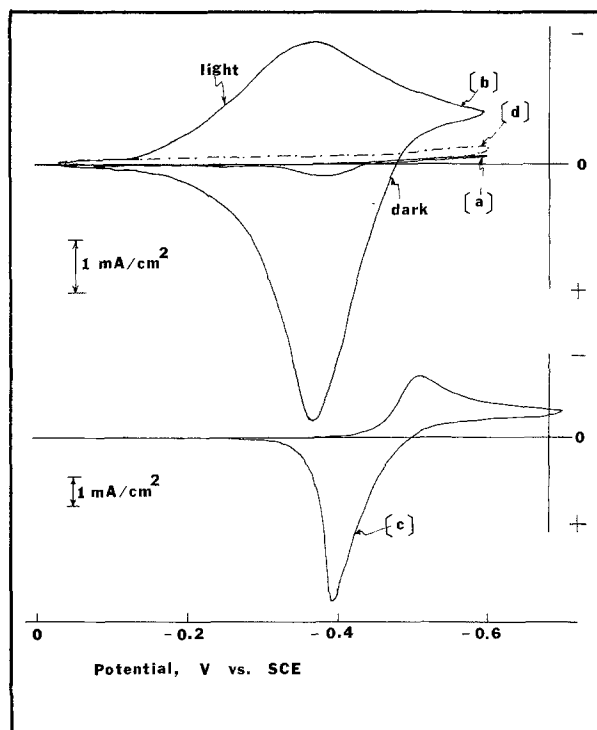

Fig. 1. Cyclic voltammograms recorded with p-GaAs at 100 mV/sec with aqueous solution containing 0.01M HVBr$_2$ and 0.2M KBr: (a) in the dark; (b) under illumination; (c) cyclic voltammogram recorded with the same solution on a Pt disk electrode (100 mV/sec); (d) cyclic voltammogram recorded with p-GaAs in solution containing only 0.2M KBr. Light source, 450W Xe lamp.
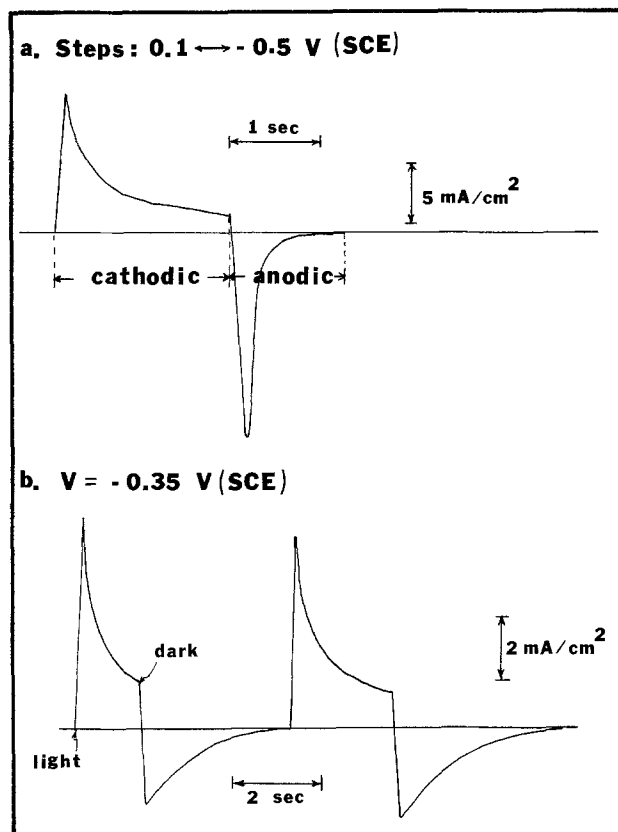

Fig. 2. Current-time transients in potential step experiments on p-GaAs in solution containing 0.01M HVBr$_2$ and 0.2M KBr: (a) potential stepped between —0.5-+0.1V under constant illumination; (b) the potential held at —0.35V *vs.* SCE under chopped illumination. Light source, 450W Xe lamp.

The cyclic voltammograms of the solution of $0.01M$ HV^{2+} dibromide and $0.2M$ KBr at a Pt electrode is shown in Fig. 1c. By comparison of this voltammogram with that obtained with p-GaAs under illumination, one can see that significant photoreduction of HV^{2+} can occur on p-GaAs at potentials ~400 mV less negative than on Pt. The photocurrent attributable to the reduction of protons on the p-GaAs in a KBr solution not containing HV^{2+} was very small (Fig. 1d). Photoreduction of HV^{2+} was also investigated with a p-GaP photocathode. In this case, the underpotential for the reduction process was even larger than in the case of p-GaAs, but the process was not very reversible and the back oxidation occurred only at more positive potentials than on a Pt electrode. Thus, upon scanning a p-GaP electrode over roughly the same potential region (Fig. 3), a gradual accumulation of HVBr occurred on the electrode surface and the cathodic current gradually decreased.

With the light intensity used in the experiments described above, the photoreduction current on p-GaAs was limited by the rate of diffusion of HV^{2+} to the electrode surface, as demonstrated by the proportionality of the cathodic photocurrent to the square root of the scan rate, v (Fig. 4). Moreover, as shown in Fig. 5, while the potential for photocurrent onset and the current at the foot of the wave depended upon the light intensity, at more negative potentials the maximum current was almost independent of intensity and was limited by the rate of diffusion of HV^{2+} to the electrode surface.

PEC cells.—Since the photoreduction of HV^{2+} occurs on p-GaAs with an underpotential of about 400 mV while the back-oxidation in the dark on p-GaAs occurs at the same potentials as on Pt, one can envision a sort of solar storage cell composed of a p-GaAs and another chemically reversible electrode (Fig. 6). This counterelectrode should have a redox potential between the potential for the photoreduction of HV^{2+} on p-GaAs and the potential for oxidation of HVBr in the dark (Fig. 6c). In such a cell, when light irradiates the p-GaAs, it is the cathode of the cell and HVBr precipitates (Fig. 6a). The HVBr precipitate on the p-GaAs is stable at open circuit, and can be oxidized in the dark back to the original HV^{2+}, while the counterelectrode becomes the cathode of the cell (Fig. 6b). Three counterelectrodes with redox potentials suitable for such a photocell, Cu/Cu-oxide, $H_xNb_2O_5/Nb_2O_5$, and Ni/Ni-oxide, were used. The open-circuit voltages, and the short-circuit currents of such cells composed of p-GaAs, and the three counterelectrodes under periodic illumination are shown in Fig. 7. The relative polarity of the p-GaAs shows the expected changes (Fig. 6) as the semiconductor is subjected to the chopped beam. In
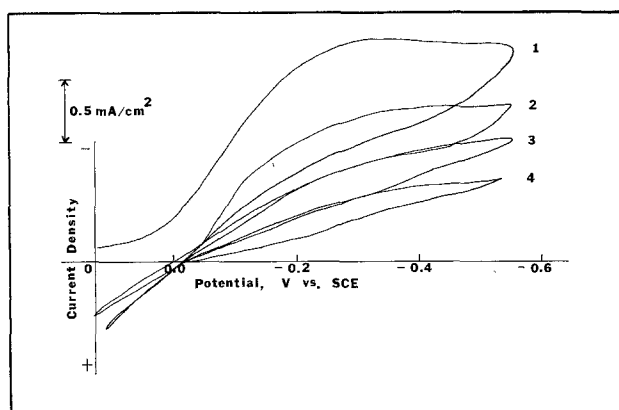

Fig. 4. Scan rate v dependence of the peak cathodic photocurrent at irradiated p-GaAs in a solution containing 0.1M HVBr$_2$ and 0.2M KBr. Light source, 450W Xe lamp.
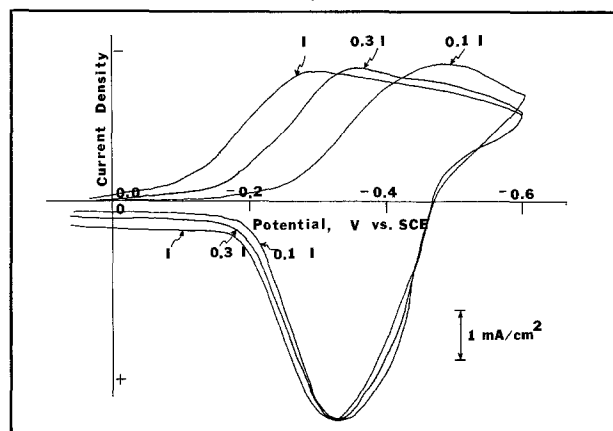
Fig. 5. Cyclic voltammograms at p-GaAs in soution of Fig. 4 with different relative light intensities. Light source, 450W Xe lamp.

the photocharged condition, the HVBr remained on the electrode surface and the open-circuit voltage was stable for at least 2 hr. The maximum open-circuit voltages were found with the Cu counterelectrode with potential excursions of up to 0.4V observed (Fig. 7A). The short-circuit currents of these cells are shown in Fig. 7B. In the light, current flows in the external circuit during which precipitation of the purple HVBr on the surface of the p-GaAs occurs. The current decays almost to zero in about 10 sec because a thick opaque film of HVBr builds up on the electrode surface and the HV^{2+} concentration is depleted near the electrode surface. The cell can be regarded as a storage battery. The precipitate of HVBr can be stored on the p-GaAs, and then oxidized in the dark to yield a current in a direction opposite to that observed under illumination. Obviously, the capacity of such a cell is very small; the maximum charge in the form of HVBr which can precipitate on the p-GaAs before the current drops to zero is about 10 mC/cm². Alternately, the cell can be considered as a type of a-c device under periodic illumination. In this mode the p-GaAs cell performance was very stable with all three cells and no deteriora-

Fig. 3. Consecutive cyclic voltammograms at irradiated p-GaP solution containing 0.01M HVBr$_2$ and 0.2M KBr. Scan rate, 100 mV/sec. Light source, 450W Xe lamp.
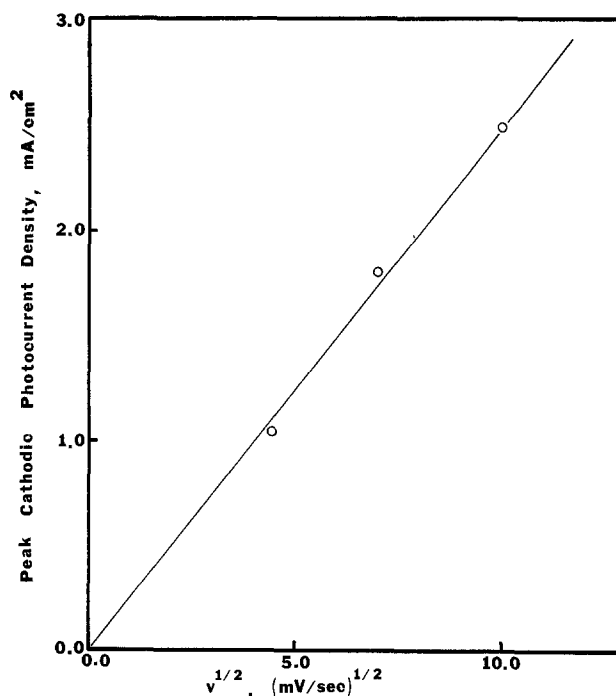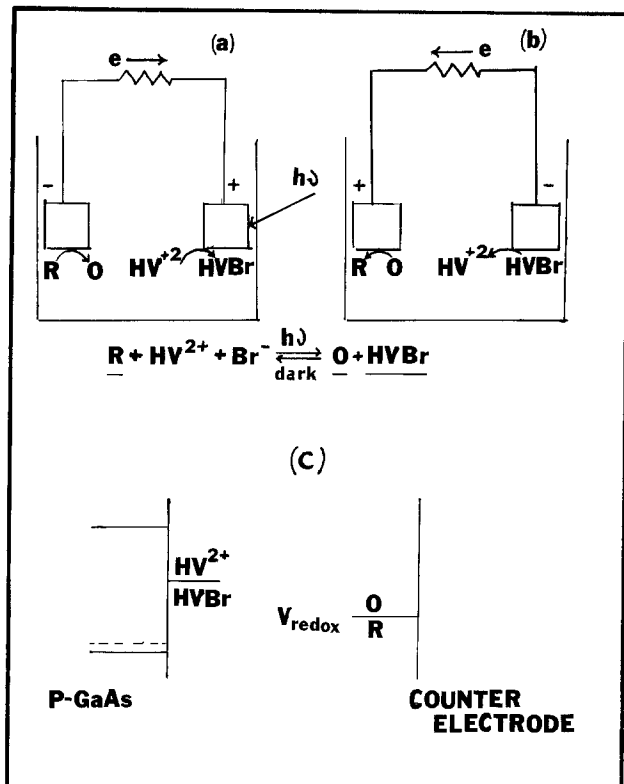
Fig. 6. Schematic description of the HVBr$_2$-based photoelectrochemical cell operating: (a) under illumination (photocharge); (b) in the dark (discharge); (c) relative energy levels and potentials at the counterelectrode, and at the p-GaAs, required for operation of the cell shown in (a) and (b).
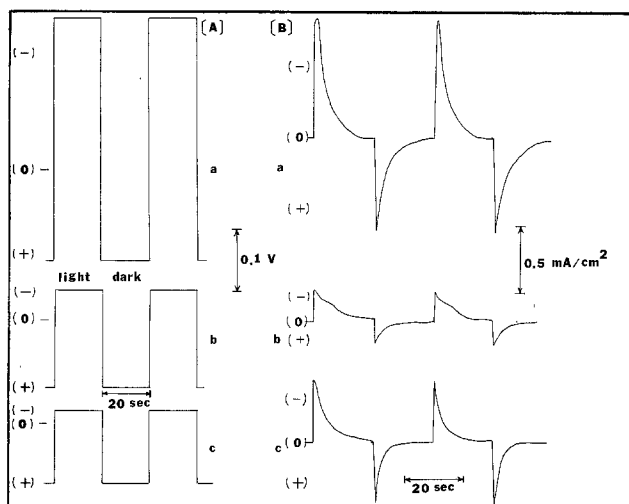

Fig. 7. (A) Open-circuit potentials and (B) short-circuit current under chopped illumination for the cells: (a) p-GaAs/HVBr/HVBr$_2$, KBr/Cu; (b) p-GaAs/HVBr/HVBr$_2$, KBr/Nb$_2$O$_5$; (c) p-GaAs/HVBr/HVBr$_2$, KBr/Ni. Light source, 450W Xe lamp.

Fig. 8. Initial short-circuit photocurrents for the three cells described in Fig. 7 as a function of light intensity (He-Ne laser).

tion or decrease in the current was observed after 4 days of continuous operation with 20 sec period illumination by the 450W xenon lamp. The open-circuit voltage, the current, and the amount of charge involved were all reproducible and stable to within 10%. The variation of the initial short-circuit current on light intensity under irradiation with the He-Ne laser (1.6 mW power) was examined with all three cells (Fig. 8). A linear dependence of the short-circuit current on light intensity was observed at the lower intensity levels. In the case of Cu counterelectrode, saturation of the current occurred at $\sim$2.5 mA/cm^2. With Ni as the counterelectrode, no saturation of the short-circuit
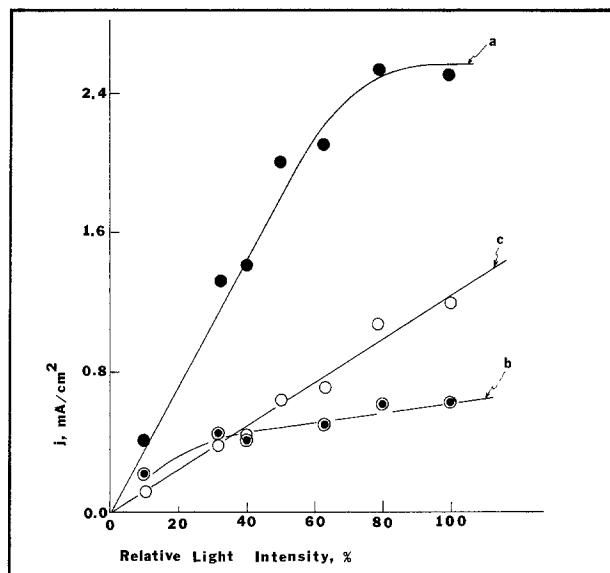
current occurred even at the highest intensity used, while with Nb$_2$O$_5$ as a counterelectrode a linear dependence was observed only at very low light levels. In all cases, the currents obtained were the highest for the Cu electrode. The current saturation observed in this case can probably be ascribed to the limitation by diffusion of HV^{2+} to the p-GaAs surface, since the magnitude of the saturation current density in Fig. 8a is similar to the limiting current found in the voltammograms, Fig. 1b, with identical HV^{2+} concentrations. With the Nb$_2$O$_5$ electrode, the short-circuit current reaches saturation earlier than in the case of Cu and was clearly limited by the oxidation reaction taking place on the Nb$_2$O$_5$ electrode. The maximum quantum efficiencies for the photocells were calculated from the slopes of the linear portions of the curves in Fig. 8, yielding values of $\sim$20% (Cu), $\sim$10% (Ni), and 2% (Nb$_2$O$_5$).

Discussion

The behavior of the p-GaAs/solution interface and a rationalization of the observed PEC cell behavior can be presented in terms of the surface controlled model for GaAs proposed elsewhere (26) (Fig. 9). In this model, the Fermi level of the semiconductor is pinned by surface states located about one-third of the way up in the gap (*i.e.*, $\sim$0.4-0.5V above the valence bandedge) (Fig. 9a). The maximum open-circuit photopotential, V_{on}, observed under intense illumination would then be $\sim$0.4V, and the open-circuit photovoltage would be the difference between V_{on} and V_{redox} of the counterelectrode reaction (Fig. 9b). In the dark after deposition of HVBr, oxidation of HVBr occurs via the surface states and the p-GaAs essentially behaves as an inert contact to the layer (Fig. 9c). The counterelectrode in a two-electrode PEC cell must have a redox potential between V_{on} and that of the HV^{2+}/HVBr system, so that only couples in a relatively narrow range of potentials are suitable.

Storage cells based on this type of electrode reaction will necessarily have small capacities, unless films which deposit on the electrode surface can be found which are both transparent to the wavelengths absorbed by the semiconductor and are electrical conductors. Moreover, higher concentrations of the soluble form are required to prevent mass transfer limitations to the photocurrent even before film formation causes current decay. Such cells may, however, find application in very low capacity batteries or as a-c devices under periodic illumination.
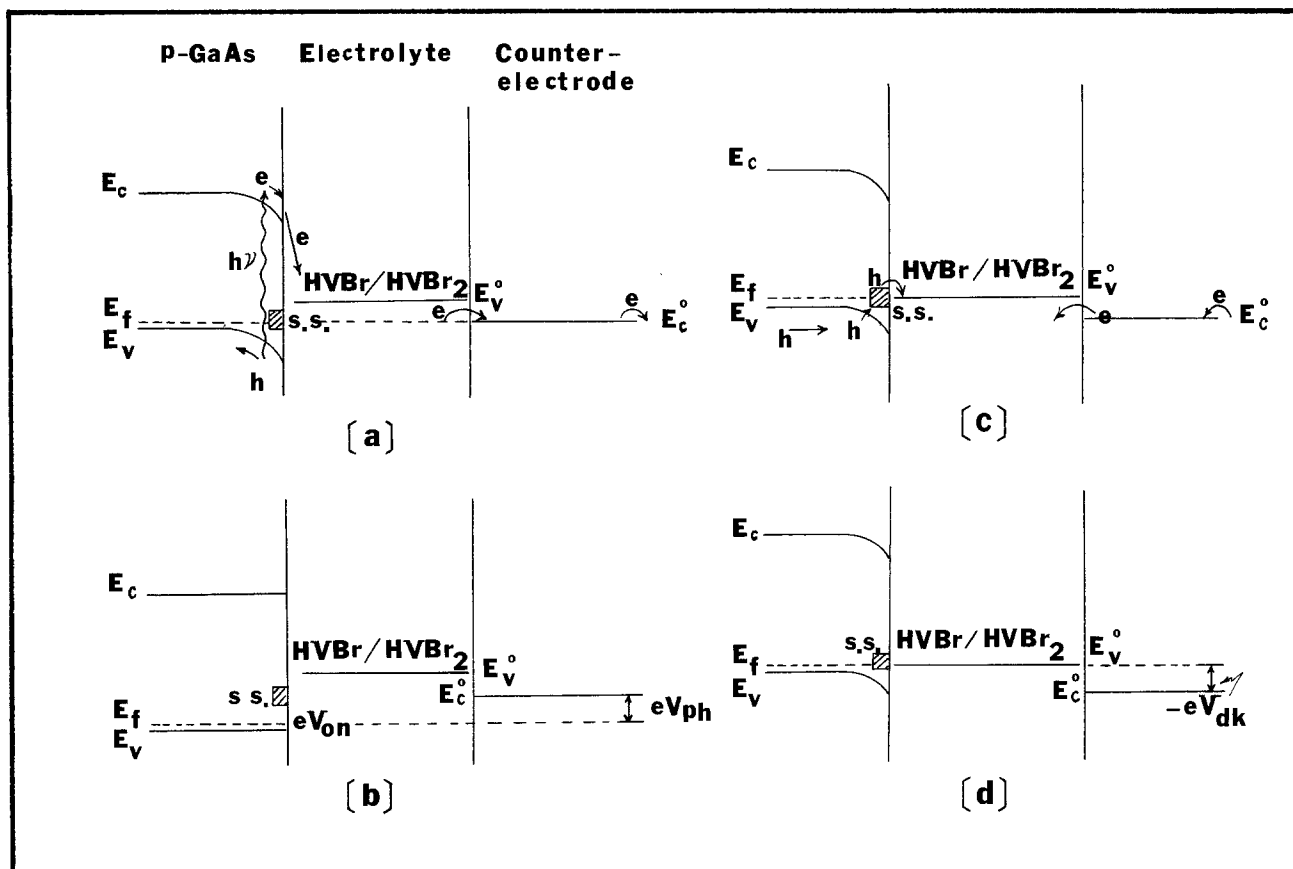
Fig. 9. Schematic description of the energy levels of the $HVBr_2$-based photoelectrochemical cells in the light at (a) short circuit, no HVBr film on p-GaAs initially, and (b) open circuit, no HVBr film on p-GaAs initially. In the dark at (c) short circuit, with HVBr film on p-GaAs, and (d) open circuit, with HVBr film on p-GaAs. E_c = conduction bandedge of p-GaAs; E_f = Fermic energy of p-GaAs; E_V = valence bandedge of p-GaAs; s.s. = surface state; E_V^0 = energy corresponding to the redox potential of heptyl viologen couple; E_C^0 = energy corresponding to the redox potential of the counterelectrode; V_{ph} = open-circuit voltage in the light; V_{dk} = open-circuit voltage in the dark; V_{on} = onset potential of photocurrent.

The application of such a system to produce a display addressable both optically and electrically (a photoelectrochromic display) is perhaps of greater interest (Fig. 10). One can envision the operation of such a device in which a light beam produces a raster on the electrode surface, and the electrode potential is switched to (i) the deposition potential (coloring), (ii) open circuit (hold), or (iii) the stripping potential (erase). The advantage of such a display, compared to the more familiar electrochromic ones, is that only two leads need be provided to the cell rather than the multiple leads and complicated electrical addressing required for a large screen or multi-character display. While the contrast ratio for HVBr on GaAs is not very good, in principle a wide bandgap semiconductor (e.g., > 3 eV), which would appear white and would be addressed with an ultraviolet beam could be employed. For a display involving rapid scanning, a system with a faster response time is also required. Similar concepts involving semiconductors and metal depositions for photoimaging have been reported (24, 27).

Acknowledgment

Any discussion of this paper will appear in a Discussion Section to be published in the December 1980 JOURNAL. All discussions for the December 1980 Discussion Section should be submitted by Aug. 1, 1980.
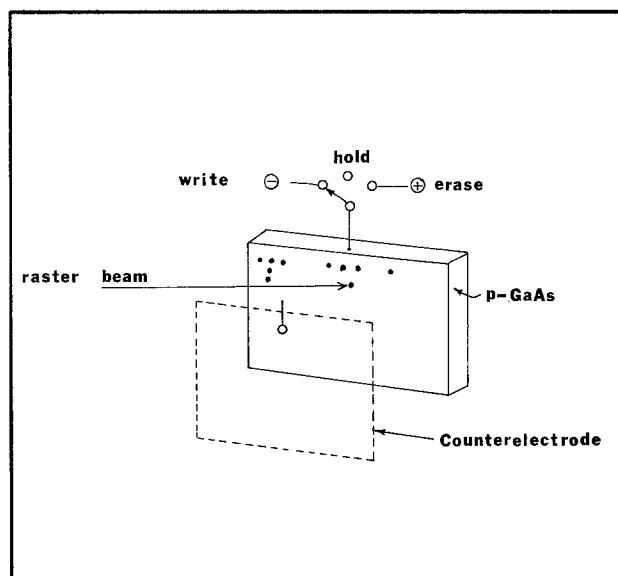

Fig. 10. Schematic description of a photoelectrochromic display device based on $HVBr_2$ reduction on p-GaAs electrode.

REFERENCES

1. R. Memming, in "Electroanalytical Chemistry," Vol. 11, A. J. Bard, Editor, pp. 1-84, Marcel Dekker, New York (1979).
2. A. J. Nozik, *Ann. Rev. Phys. Chem.*, **29**, 189 (1978).
3. H. Gerischer, *J. Electroanal. Chem.*, **58**, 263 (1979).
4. A. J. Bard, *J. Photochem.*, **10**, 59 (1979).

5. D. Laser and A. J. Bard, *This Journal*, **123**, 1027 (1976).
6. T. Inoue, T. Watanabe, A. Fujishima, K. Honda, and K. Kohayakawa, *ibid.*, **124**, 719 (1977).
7. A. B. Ellis, J. M. Bolts, S. W. Kaiser, and M. S. Wrighton, *J. Am. Chem. Soc.*, **99**, 2848 (1977).
8. R. Memming, in "Proceedings of Conference on Electrochemistry and Physics of Semiconductor-Liquid Interface under Illumination," A. Heller, Editor, pp. 38-48, Airlie, Virginia.
9. J. M. Bolts, A. B. Ellis, K. D. Legg, and M. S. Wrighton, *J. Am. Chem. Soc.*, **99**, 4826 (1977).
10. G. Hodes, J. Manassen, and D. Cahen, *Nature*, **261**, 403 (1976).
11. J. Manassen, G. Hodes, and D. Cahen, *This Journal*, **124**, 533 (1977).
12. R. N. Noufi, P. A. Kohl, and A. J. Bard, *ibid.*, **125**, 375 (1978).
13. P. A. Kohl and A. J. Bard, *ibid.*, **126**, 59, 603 (1979).
14. B. A. Parkinson, A. Heller, and B. Miller, *ibid.*, **126**, 954 (1979).
15. R. Memming, *ibid.*, **125**, 117 (1978).
16. H. Yoneyama, H. Sakamato, and H. Tamura, *Electrochim. Acta*, **20**, 341 (1975).
17. R. E. Malpas, K. Itaya, and A. J. Bard, *J. Am. Chem. Soc.*, **101**, 2535 (1979).
18. M. Tomkiewicz and J. M. Woodall, *This Journal*, **124**, 1436 (1977).
19. P. A. Kohl and A. J. Bard, *ibid.*, **126**, 59 (1979).
20. C. J. Schoot, J. J. Ponjee, H. T. Van Dam, R. A. Van Doorn, and P. T. Bolneijn, *Appl. Phys. Lett.*, **23**, 64 (1973).
21. R. J. Jasinski, *This Journal*, **124**, 637 (1977).
22. J. Bruinind and C. G. A. Kregting, *ibid.*, **125**, 1397 (1978).
23. J. D. Luttmer and A. J. Bard, *ibid.*, **126**, 414 (1979).
24. T. Inoue, A. Fujishima, and K. Honda, *Chem. Lett.*, **11**, 1197 (1978).
25. M. Yamana, *Appl. Phys. Lett.*, **29**, 571 (1976).
26. Fu-Ren F. Fan and A. J. Bard, *J. Am. Chem. Soc.*, Submitted.
27. G. L. McLeod, *Photogr. Sci. Eng.*, **13**, 93 (1969).

Semiconductor Electrodes

XXIII. The Determination of Flatband Potentials from Differential Stress Measurements with Attached Piezoelectric Detectors

Lee J. Handley and Allen J. Bard*

Department of Chemistry, The University of Texas at Austin, Austin, Texas 78712

ABSTRACT

A new method for the determination of the flatband potential, V_{fb}, of semiconductor electrodes by differential stress measurements of a piezoelectric detector bonded to the semiconductor is reported. Values of V_{fb} for single crystal n-$SrTiO_3$ and p-GaAs, and polycrystalline n-TiO_2 in 1N NaOH and 1N H_2SO_4 are shown to be in good agreement with previously determined values. Possible application of such measurements to the study of surface changes and breakdown is suggested.

The flatband potential, V_{fb}, of a semiconductor/electrolyte solution interface is an important parameter in explaining the electrochemical characteristics of the system in the dark and under illumination (1-3). V_{fb} is a function of both the semiconductor material and the solution composition, and is measured to determine the locations of the semiconductor valence and conduction bandedges with respect to solution energy levels. Usually V_{fb}-values are determined by direct measurements of the space charge differential capacity, C_{sc}, (Schottky-Mott plots) or by determinations of the open-circuit photopotential (or the potential for the onset of the photocurrent) under intense irradiation. Both of these methods often suffer from difficulties which result in large uncertainties in the V_{fb}-values estimated by them. In C_{sc} measurements the Schottky-Mott plots are frequently nonlinear and yield V_{fb}-values which are functions of the frequency used. This has been attributed to the effect of surface states and other factors (4). The estimation from photopotentials can also be perturbed by the existence of surface states or intermediate levels as well as by recombination effects which, for an n-type semiconductor, will yield onset photopotentials less negative than the actual V_{fb}-value (5).

V_{fb} can also be determined by observing the voltammetric response in the dark of couples spanning a potential range above and below V_{fb} (5, 6). Such measurements usually yield a V_{fb}-value with considerable uncertainty and may also be perturbed by electron transfers occurring via surface states. In this paper, we

propose a method for the determination of V_{fb}, based on the measurement of differential stress (with a piezoelectric crystal attached to the semiconductor electrode) as a function of potential, which is experimentally simple and theoretically direct.

There have been several previous reports of the application of piezoelectric materials (which are materials which produce a potential when placed under a stress) to measurements at metal electrodes (7-10).

From a modified form of the Lipmann equation that was used by Gokhstein (7) for metal electrodes, the differential surface stress $(\partial \sigma_s/\partial E)$ is related to the surface charge density (q) and deformation by

$$\partial \sigma_s/\partial E = -q - \partial q/\partial \theta \qquad [1]$$

where θ is the ratio of the surface area before and after deformation. For an ideally polarized electrode, the term $\partial q/\partial \theta$ is zero, since the charge density does not depend upon the deformation of the electrode surface. Even for nonpolarizable electrodes this term may be small and is equal to zero at the flatband potential, because at V_{fb} there is no charge on the electrode.

For semiconductor electrodes, the excess charge q is distributed in the space charge region. At potentials negative of the flatband potential, the space charge region has an excess of electrons and the differential stress measurements will be positive. At the flatband potential there is no excess charge and the differential stress is zero. For potentials positive of the flatband potential there is an accumulation of holes in the space charge region and the differential stress will be negative. Thus, as implied by Eq. [1], the differential stress tracks the space charge, and the intercept of the dif-